GMR
The Original

SUSTAINABLE GREEN FABRICATION OF STARCH/PVA/CUO ELECTROSPUN NANOFIBERS USING ECTOCARPALES (MARINE MACROALGAE) EXTRACT: PHYSICOCHEMICAL CHARACTERIZATION AND ANTIDIABETIC EVALUATION

Vasundhara Chandirasekar[1], Akilesh Anbalagan[2], Shanmuga Priya Vimalan[3], Alagendran Subbarayalu[4], Kaliyamoorthy Dass[5*]

[1]Saveetha Medical College & Hospital (SMCH), Saveetha Institute of Medical and Technical Sciences (SIMATS), Thandalam, Chennai, Tamil Nadu 602105, India. Email: srinidhirajaraman04@gmail.com
[2]Department of Anaesthesia, Saveetha Medical College and Hospital, Saveetha Institute of Medical And Technical Sciences (SIMATS), Thandalam, Chennai-602105, Tamil Nadu, India. Email: dr.akilesh97@gmail.com; ORCID: https://orcid.org/0009-0008-3742-6538
[3]Department of Chemistry, School of Basic Sciences, Vels Institute of Science Technology and Advanced Studies, Pallavaram, Chennai-600117, Tamil Nadu, India. Email: shanmugapriyavimalan@gmail.com; ORCID: https://orcid.org/0009-0004-7710-0226
[4]Saveetha College of Nursing (SCON), Saveetha Institute of Medical and Technical Sciences (SIMATS), Chennai – 602105, Tamil Nadu, India. Email: alagendrans.scon@saveetha.com; ORCID: https://orcid.org/0009-0009-0749-7180
[5]Natural Product and Vector Control Research Lab, Department of Pharmacology, Saveetha Medical College and Hospital, Saveetha Institute of Medical And Technical Sciences (SIMATS), Thandalam, Chennai-602105, Tamil Nadu, India. dass.smc@saveetha.com; kdassrsgc1987@gmail.com; ORCID: https://orcid.org/0000-0002-4564-3275

ABSTRACT

This study presents an eco-friendly approach for synthesizing copper oxide nanoparticles (CuO NPs) using Ectocarpales algal extract and their incorporation into starch/PVA nanoscaffolds for antidiabetic applications. The algal-mediated synthesis yielded crystalline, spherical CuO NPs (50–200 nm) with a monoclinic tenorite structure, as confirmed by XRD and SEM. UV-Vis spectroscopy showed characteristic absorption at 200 nm, while FT-IR analysis revealed biomolecule-mediated stabilization. The nanoscaffolds exhibited a porous, fibrous morphology (70–90 nm fiber diameter) with uniform NP dispersion. Thermal analysis demonstrated stability up to 337°C, and zeta potential measurements indicated moderate colloidal stability (+14.03 mV). Antidiabetic activity was evaluated through α-amylase and α-glucosidase inhibition assays. The algal extract showed moderate inhibition (18.72–53.92%), while CuO NPs exhibited enhanced efficacy (20.72–68.92%). The nanoscaffolds demonstrated superior performance (23.72–81.92%), approaching the standard drug acarbose, likely due to synergistic effects between CuO NPs and the polymer matrix. These results highlight the potential of algal-synthesized CuO NPs and their nanocomposites as sustainable, high-performance antidiabetic agents. The study provides insights into green nanotechnology for biomedical applications, warranting further in vivo investigations for therapeutic validation.

KEYWORDS: Ectocarpales, Green synthesis, CuO nanoparticles, Starch/PVA/CuO-NPs nanoscaffolds, Antidiabetic activity.

1. INTRODUCTION

Diabetes mellitus has emerged as one of the most challenging global health crises of the 21st century, with the International Diabetes Federation projecting that 783 million people will be affected by 2045 [1]. This metabolic disorder, characterized by chronic hyperglycemia resulting from insulin deficiency or resistance, necessitates innovative therapeutic approaches to complement existing treatments [2]. Current pharmocological interventions, particularly α-glucosidase and α-amylase inhibitors like acarbose, often present undesirable side effects including gastrointestinal disturbances, highlighting the urgent need for safer alternatives [3]. In this context, nanotechnology and natural product research have converged to offer promising solutions, with particular emphasis on green-synthesized metal oxide nanoparticles and their nanocomposites [4]. The exploration of marine algae as a source of bioactive compounds has gained significant momentum in recent years[5]. Among these, brown algae from the Ectocarpales order have demonstrated remarkable potential due to their rich content of polyphenols, flavonoids, and polysaccharides [6]. These secondary metabolites not only exhibit inherent biological activities but also serve as excellent reducing and stabilizing agents in nanoparticle synthesis [7]. The choice of Ectocarpales species from the Rameswaram coastline is particularly strategic, as marine organisms from this biodiverse region have been shown to possess unique phytochemical profiles shaped by their specific environmental conditions, including high salinity and intense solar radiation [8].

Copper oxide nanoparticles (CuO NPs) have attracted considerable attention in biomedical applications due to their distinctive properties, including high surface area-to-volume ratio, tunable morphology, and exceptional catalytic activity [9]. Compared to other metal oxides, CuO NPs demonstrate superior biocompatibility and cost-effectiveness while maintaining excellent therapeutic potential [10]. Traditional physical and chemical synthesis methods often involve toxic

reagents and generate hazardous byproducts, making green synthesis approaches using algal extracts an environmentally sustainable alternative [11]. This biological synthesis route not only reduces environmental impact but also enhances the biocompatibility and functionality of the resulting nanoparticles through natural capping agents [12].

The development of nanocomposite scaffolds represents a significant advancement in drug delivery systems for diabetes management [13]. Starch and polyvinyl alcohol (PVA) have emerged as ideal polymeric matrices due to their excellent film-forming properties, biodegradability, and biocompatibility[14]. When combined with CuO NPs, these polymers create a synergistic system that potentially enhances therapeutic efficacy while minimizing side effects [15]. The electrospinning technique employed in this study allows for the fabrication of nanofibrous mats with high porosity and surface area, mimicking the extracellular matrix and facilitating controlled release of active components [16]. This approach addresses critical challenges in antidiabetic drug delivery, including poor solubility, low bioavailability, and non-specific distribution of conventional formulations.

The inhibition of carbohydrate-hydrolyzing enzymes, particularly α-amylase and α-glucosidase, has been established as an effective strategy for managing postprandial hyperglycemia in type 2 diabetes [17]. These enzymes play pivotal roles in starch digestion and glucose absorption in the small intestine [18]. While current inhibitors like acarbose and miglitol effectively reduce post-meal glucose spikes, their use is often limited by adverse effects [19]. Nanomaterial-based inhibitors offer several advantages, including enhanced stability, targeted action, and the potential for combination therapies [20]. The unique surface chemistry and quantum effects of CuO NPs may enable more efficient enzyme inhibition through multiple mechanisms, including direct interaction with catalytic sites and alteration of enzyme conformation [21].

Recent advances in characterization techniques have provided unprecedented insights into the properties of biogenic nanoparticles and their composites. UV-Visible spectroscopy serves as a primary tool for confirming nanoparticle formation through surface plasmon resonance analysis [22]. Fourier-transform infrared spectroscopy (FTIR) enables the identification of functional groups involved in nanoparticle synthesis and stabilization [23]. X-ray diffraction (XRD) provides crucial information about crystallinity and phase composition [24], while scanning electron microscopy (SEM) offers detailed morphological characterization [25]. Thermal analysis and zeta potential measurements further contribute to understanding the stability and behavior of these nanomaterials in biological systems [26].

The rationale for this study stems from several critical gaps in current research. While numerous studies have investigated the biological activities of algal extracts or synthetic nanoparticles separately, few have explored the combined potential of algal-synthesized nanoparticles embedded in polymeric nanoscaffolds for diabetes management. Furthermore, most existing research on nanomaterial-based enzyme inhibitors has focused on gold or silver nanoparticles, with limited attention given to copper oxide systems despite their cost advantages and comparable efficacy [27]. The coastal ecosystem of Rameswaram remains underexplored for its algal biodiversity and associated biotechnological potential, particularly in the context of nanomaterial synthesis [11].

This research aims to develop a comprehensive solution that addresses multiple aspects of diabetes management: (1) utilizing an environmentally benign synthesis approach for CuO NPs using Ectocarpales algal extract, (2) fabricating starch/PVA nanoscaffolds incorporating these nanoparticles through electrospinning, (3) thoroughly characterizing the physicochemical properties of both nanoparticles and nanocomposites, and (4) evaluating their antidiabetic potential through systematic in vitro enzyme inhibition assays. The study employs a multidisciplinary approach combining phycology, nanotechnology, materials science, and biochemical pharmacology to develop a novel therapeutic platform.

The significance of this work extends beyond its immediate application in diabetes treatment. It demonstrates the potential of marine resources in sustainable nanotechnology, contributes to the development of green chemistry protocols, and provides a model for the rational design of nanocomposite therapeutic systems [28]. From a clinical perspective, the developed nanoscaffold system offers potential advantages such as controlled release kinetics, reduced dosing frequency, and minimized side effects compared to conventional antidiabetic drugs [29]. The findings may also have implications for other therapeutic areas where enzyme inhibition is desired, such as obesity management or anticancer therapies.

2. MATERIALS AND METHODS

2.1. Chemicals and materials

This investigation employed marine brown algae from the Ectocarpales order, collected from Rameswaram, Tamil Nadu, as a green source for synthesizing CuO NPs. Copper (II) sulfate pentahydrate ($CuSO_4 \cdot 5H_2O$, Sigma-Aldrich) served as the metal precursor. PVA (molecular weight ~145,000) and commercially available starch were utilized to prepare nanofibers via electrospinning using a HOLMARC HO-NFES-040 setup. All other solvents and chemicals used in the experiments were of analytical grade, sourced from Sigma-Aldrich and Merck, and were used without additional purification. Analytical techniques included UV–visible spectroscopy, Fourier-transform infrared spectroscopy (FT-IR), X-ray diffraction (XRD) using the Bruker D8 Advance, scanning electron microscopy (SEM) via JEOL JSM-IT800, zeta potential measurements using a Malvern Zetasizer Ultra, and thermal analysis through a PerkinElmer TGA 8000. Antidiabetic assessments were performed α-amylase and α-glucosidase inhibition Assays.

2.2. Collection and preparation of Ectocarpales algae

Brown macroalgae specimens belonging to the Ectocarpales order were manually gathered from the intertidal zones along the Rameswaram coastline. To ensure purity, the samples underwent a multistep cleaning process: first rinsed with tap water to remove debris and sand, followed by a wash with distilled water to eliminate residual impurities. Cleaned algal biomass (~100 g) was finely chopped and shade-dried at room temperature (approximately 28°C) for two weeks. The

completely dried biomass was then ground into a uniform powder using a mechanical grinder and stored in moisture-free containers for later use.

2.3. Ultrasound-assisted extraction of bioactives

For extracting bioactive constituents, 2 g of the powdered algae were suspended in 50 mL of Milli-Q water in a sterile beaker. The mixture was exposed to ultrasonication in a LABQUEST bath (Borosil; Serial No. 941032329018) maintained at 60°C for 45 minutes. Ultrasonic waves facilitated the disruption of algal cell walls, promoting the release of intracellular phytochemicals. The resultant mixture was filtered using Whatman No. 1 filter paper under sterile conditions. The filtrate was collected in a clean container and kept at 10°C for immediate use or lyophilized for long-term storage, yielding a dry powdered extract for further application [30, 31].

2.4. Green synthesis of CuO NPs

CuO NPs were synthesized through a bio-reduction method using the algal extract. A 0.1 M solution of $CuSO_4 \cdot 5H_2O$ (50 mL) was combined with 10 mL of the algal extract (prepared by dissolving 10 mg of lyophilized powder in 10 mL Milli-Q water) in a 5:1 volume ratio. This solution was stirred magnetically at 650 rpm at 60°C for 2 hours. A visible change from deep blue to a pale bluish-green color indicated CuO nanoparticle formation. The colloidal product was washed thrice with double-distilled water to eliminate residual phytochemicals and unreacted ions. The purified nanoparticles were lyophilized for 48 hours to obtain a stable CuO nanopowder for subsequent characterization and integration into scaffolds [32].

2.5. Fabrication of starch/PVA nanofibers with CuO NPs

Hybrid nanofibrous mats were created by dissolving 15% (w/w) PVA in distilled water with continuous heating and stirring. Once dissolved, 100 mg of starch and 100 mg of biosynthesized CuO NPs were incorporated into the polymer solution. The mixture was stirred at 50°C for 2.5 hours to ensure even dispersion. Electrospinning was conducted using the HOLMARC HO-NFES-040 system. The polymer blend was loaded into a syringe fitted with a 0.84 mm needle. The optimized electrospinning parameters included an applied voltage of 11.5 kV, a nozzle-to-collector distance of 12.3 cm, and a feed rate of 0.4 mL/h. Fibers were collected onto aluminium foil for 6 to 8 hours at ambient conditions, forming uniform nanofibrous mats [33-35].

2.6. Physicochemical characterization techniques

2.6.1. UV–Visible spectral analysis

The optical behavior of the algal extract, CuO NPs, and nanofiber composites was analyzed using a VIS SPEC V-730 spectrophotometer. Absorbance spectra were recorded from 200 to 800 nm using deionized water as the blank reference [36].

2.6.2. FT-IR Spectroscopy analysis

FT-IR analysis was performed on a PerkinElmer Spectrum Two system in ATR mode. Spectra were recorded between 4000 and 400 cm^{-1} at a resolution of 4 cm^{-1}. Sixty-four scans were averaged for each sample to enhance spectral quality and detect functional group interactions during nanoparticle synthesis and scaffold incorporation [37].

2.6.3. XRD analysis

XRD was employed to determine the crystalline nature of the synthesized materials. Measurements were carried out using a Bruker D8 Advance diffractometer equipped with CuKα radiation ($\lambda = 1.5406$ Å), operated at 40 kV and 40 mA. Scans ranged from 5° to 90° (2θ) at a step size of 0.029649°, allowing phase identification of both nanoparticles and composite fibers [38].

2.6.4. SEM analysis

The surface structure and morphology of CuO NPs and electrospun fibers were examined with a JEOL JSM-IT800 SEM. Samples were coated with a fine gold layer to enhance image resolution and conductivity. SEM micrographs were assessed for fiber alignment, nanoparticle distribution, and surface uniformity [39].

2.6.5. TGA

Thermal stability was evaluated using a PerkinElmer TGA 8000 analyzer. Around 5 mg of sample was heated from room temperature to 550°C at 15°C/min under a nitrogen flow. The degradation patterns were analyzed to determine thermal transitions and compositional stability [40].

2.6.6. Particle size and zeta potential

Dynamic light scattering (DLS) and electrophoretic light scattering were used to determine particle size distribution and zeta potential using a Malvern Zetasizer Ultra. These measurements provided insights into the dispersion behavior and colloidal stability of the green-synthesized nanoparticles [41].

Supporting data are accessible at Mendeley Data (DOI: 10.17632/m7jzmb7mr9.1).

2.7. Evaluation of antidiabetic properties

2.7.1. Inhibition of α-amylase activity

The α-amylase inhibition capacity of the algal extract, CuO NPs, and composite nanoscaffolds was assessed using a modified DNSA method [42]. A mixture of 200 µL of α-amylase (1 U/mL) and 200 µL of each sample (25–100 µg/mL) was incubated at 37°C for 10 minutes. Subsequently, 200 µL of 1% starch solution (in 0.02 M phosphate buffer, pH 6.9) was added and incubated for 30 minutes. The reaction was stopped with 400 µL of DNSA reagent and heated for 5 minutes

in a water bath. Absorbance was read at 540 nm. Acarbose served as the standard. The percentage inhibition and IC_{50} values were determined using non-linear regression [43].

2.7.2. Inhibition of α-glucosidase activity

A colorimetric assay using p-nitrophenyl-α-D-glucopyranoside (pNPG) was conducted to assess α-glucosidase inhibition [44]. In this assay, 50 µL of α-glucosidase (1 U/mL) was incubated with 50 µL of each test concentration (25–100 µg/mL). The reaction and subsequent absorbance measurements followed standard protocols to determine inhibitory efficacy [36, 45].

3. RESULTS

3.1. UV–Visible spectroscopic characterization

The UV–Visible absorption spectra of the Ectocarpales extract and CuO NPs were recorded using a JASCO UV-VIS spectrophotometer (Model V-730), covering the spectral range of 200 to 800 nm (Figure 1.). Deionized water served as the blank control. The Ectocarpales extract showed a broad absorption band within the 200–400 nm region, peaking around 300 nm with an absorbance value of 0.93687. This peak is characteristic of π-π* electronic transitions commonly associated with phenolic constituents, flavonoids, and chlorophyll derivatives present in marine algae. A progressive decline in absorbance was noted in the 400–800 nm range, indicating limited absorption in the visible region and suggesting a low presence of extended conjugated systems.

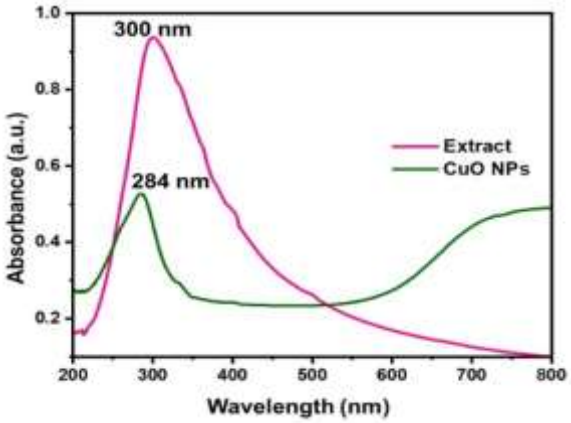

Figure 1. UV–Visible Spectroscopy analysis of algae extract and CuO NPs

In contrast, the CuO NPs exhibited a sharp absorption edge in the ultraviolet domain, with a prominent maximum at 200 nm (absorbance: 0.53295), which aligns with the intrinsic bandgap absorption and potential surface plasmon resonance phenomena. The absorbance diminished steadily across the higher wavelength range, a typical pattern for semiconducting nanomaterials. The distinct spectral differences between the algal extract and the CuO NPs support their differing compositional nature—organic for the former and inorganic for the latter. These spectral profiles confirm the successful synthesis and unique optical features of both the algal extract and the CuO NPs.

3.2. FT-IR Spectral analysis

FT-IR spectra of CuO NPs and the fabricated nanoscaffolds were recorded using a PerkinElmer Spectrum Two spectrometer in Attenuated Total Reflectance (ATR) mode, spanning 4000 to 400 cm^{-1} with a resolution of 4 cm^{-1} over 64 scans (Figure 2.). The CuO NPs spectrum showed characteristic peaks at 3216 cm^{-1}, indicating O–H stretching vibrations from adsorbed moisture, and at 1511 cm^{-1}, suggestive of C=O stretching or aromatic ring vibrations. The peak at 860 cm^{-1} was attributed to Cu–O stretching, confirming the presence of copper oxide bonds and residual organic moieties from the synthesis process.

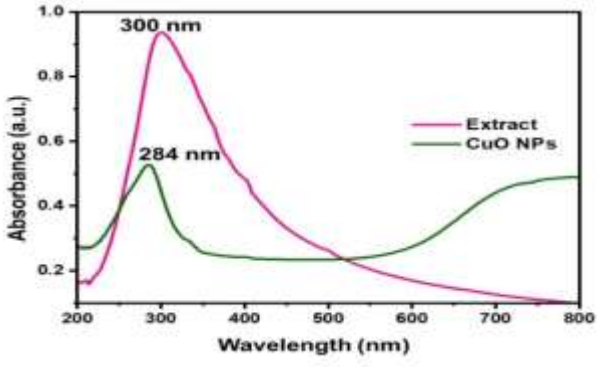

Figure 2. FTIR analysis of CuO NPs and starch/PVA/CuONPs nanoscaffolds

In comparison, the nanoscaffold spectrum revealed broader and more complex vibrational bands, with a significant peak at 3298 cm^{-1}, indicating N–H and/or O–H stretching vibrations typical of polymeric matrices. A peak at 2107 cm^{-1} was possibly due to C≡N or cumulative C=C=N functionalities. Peaks at 1652 cm^{-1} and 1327 cm^{-1} were associated with carbonyl (C=O) stretching and C–N or O–H bending vibrations, respectively. Additional bands at 840 cm^{-1} and 607 cm^{-1} suggested glycosidic linkages and possible inorganic-polymer interactions. The FT-IR data confirmed the successful formation of CuO NPs and their integration into a polymer-rich scaffold system. The differences in spectral patterns between the two samples indicate distinct chemical compositions, supporting the hybrid nature of the nanoscaffolds.

3.3. XRD analysis

XRD patterns of CuO NPs and nanoscaffolds were obtained using a Bruker D8 Advance diffractometer operating with CuKα radiation (λ = 1.5406 Å), set at 40 kV and 40 mA (Figure 3.). The scanning range covered 5°–90° (2θ) with a step size of 0.029649°. The CuO NPs demonstrated a crystalline structure, evidenced by 25 distinct diffraction peaks. Notable reflections occurred at 26.201° (d = 3.398 Å), 20.312° (d = 4.369 Å), and 36.148° (d = 2.483 Å), correlating with the monoclinic phase of CuO (tenorite), as confirmed by JCPDS card No. 05-0661. The sharpness of peaks and narrow FWHM values indicated high crystallinity.

In contrast, the nanoscaffolds exhibited 14 diffraction peaks, with major signals at 21.199° (d = 4.188 Å) and 30.844° (d = 2.897 Å), suggesting a semi-crystalline polymer structure with approximately 15.9% crystalline and 84.1% amorphous regions. Broader peaks and greater FWHM values suggested a less ordered framework, potentially caused by the dispersion of CuO NPs within the polymer. The absence of overlapping diffraction peaks confirmed the structural integrity and phase purity of both CuO NPs and nanoscaffolds.

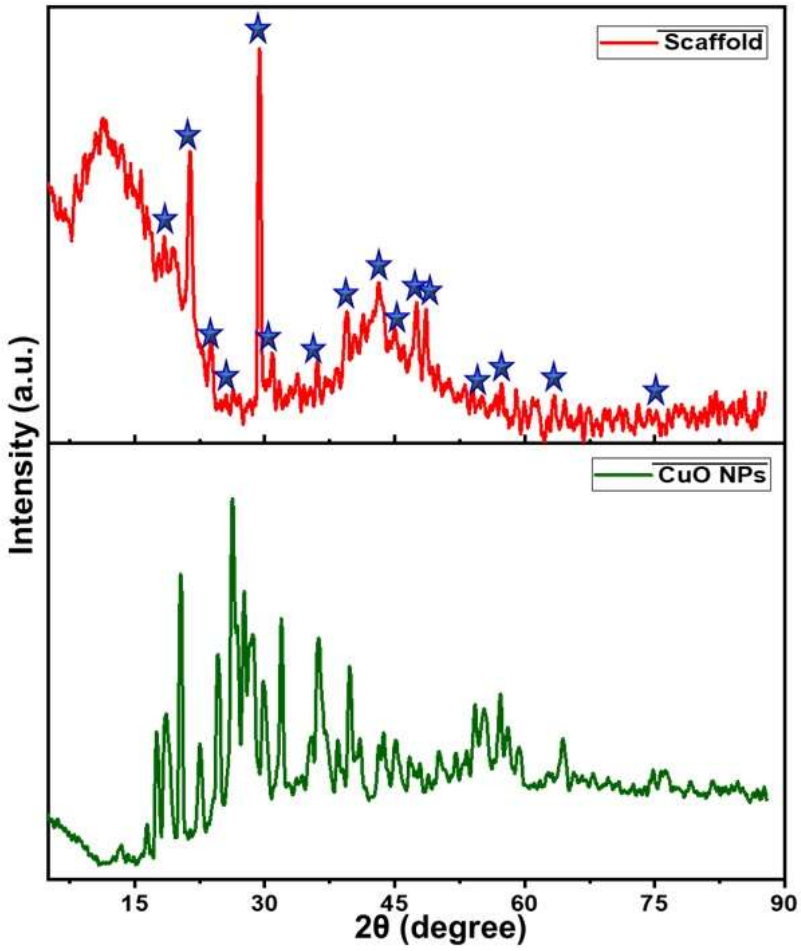

Figure 3. XRD analysis of CuO NPs and starch/PVA/CuONPs nanoscaffolds

3.4. SEM analysis

Morphological analysis using scanning electron microscopy (JEOL JSM-IT800 NANO SEM) revealed distinct surface characteristics of the synthesized CuO NPs and nanofibrous scaffolds (Figure 4.). The CuO NPs showed a generally spherical to slightly irregular shape, with diameters ranging from 50 to 200 nm. Mild agglomeration was noted, likely due to surface energy interactions, though individual particles remained discernible.

The nanoscaffolds presented a well-formed fibrous architecture, featuring an interconnected and porous network. The fiber diameters ranged between 70–90 nm, with a smooth texture and occasional bead formation, indicating optimal

electrospinning parameters. Bright nanoparticles embedded on or near the fiber surfaces suggested uniform dispersion of CuO NPs within the scaffold matrix. This composite structure, with hierarchical porosity and strong NP integration, is favorable for biomedical applications such as tissue scaffolds and wound dressings. The absence of visible aggregation further confirmed effective nanoparticle incorporation.

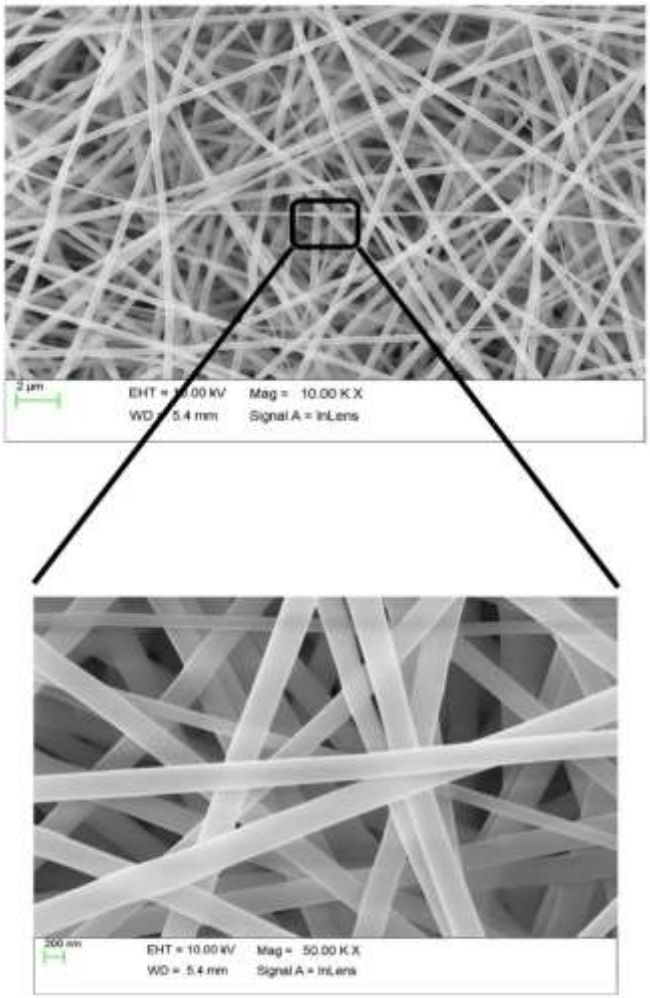

Figure 4. SEM analysis of starch/PVA/CuONPs nanoscaffolds

3.5. TGA

Thermal stability of the nanoscaffolds was evaluated via TGA using a PerkinElmer TGA 8000 system (Figure 5.). A sample mass of 1.012 mg was heated from ambient temperature to 600°C under a nitrogen atmosphere at a rate of 15°C/min. The thermogram revealed a multi-phase degradation process. The initial weight loss (3.581%) below 100°C corresponded to moisture and solvent evaporation. Major decomposition occurred at 336.92°C, indicative of breakdown of the polymer matrix (e.g., starch or PVA). The process completed around 400.84°C, with a total weight loss of 31.102%, leaving a stable inorganic residue—attributed to the CuO content.

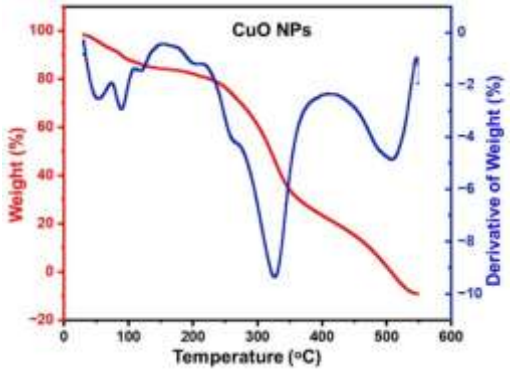

Figure 5. TGA analysis of starch/PVA/CuONPs nanoscaffolds

The high thermal decomposition point and residual mass indicate the composite's thermal robustness, essential for applications in environments involving elevated temperatures. These findings highlight the hybrid composition and structural integrity of the scaffold.

3.6. DLS and zeta potential

Particle size and surface charge of the CuO NPs were assessed using a Malvern Zetasizer Ultra. DLS measurements revealed mean hydrodynamic diameter (Z-average) was 79.8 nm (Figure 6.) with a polydispersity index (PDI) of 0.475, indicating moderate heterogeneity. Zeta potential analysis recorded an average surface charge of +14.03 mV, with two distinct populations centered at +10.94 mV and +28.06 mV (Figure 7.). These positive values suggest a cationic surface, likely due to residual biomolecules or capping agents from the biosynthesis process. The colloidal suspension showed a conductivity of 0.1179 mS/cm and a quality factor of 2.084, indicating relatively stable dispersion. Despite the presence of some large aggregates, the nanoparticles maintain sufficient colloidal stability for potential biomedical or environmental uses. These measurements provide critical insights into the surface behavior and dispersibility of the synthesized CuO NPs.

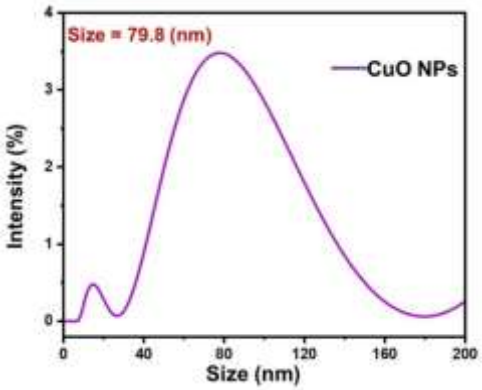

Figure 6. Particle size analysis of CuO NPs

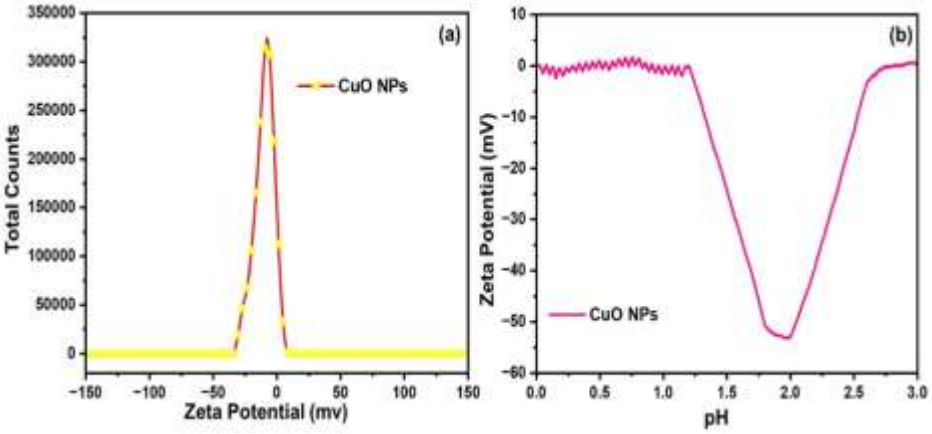

Figure 7. Zeta potential analysis of CuO NPs

3.7. Antidiabetic activity analysis

The antidiabetic activity of the algal extract, CuO NPs, and starch/PVA/CuO-NPs nanoscaffolds was evaluated through their inhibition of α-amylase and α-glucosidase enzymes (Figure 8.), which play key roles in carbohydrate digestion and glucose absorption. The results demonstrated a concentration-dependent response across all tested samples (25–100 µg/mL). The standard drug, acarbose, exhibited the highest inhibition, with values ranging from 25.13% at 25 µg/mL to 81.34% at 100 µg/mL for α-amylase and 28.13% to 84.34% for α-glucosidase, confirming its effectiveness as a reference compound.

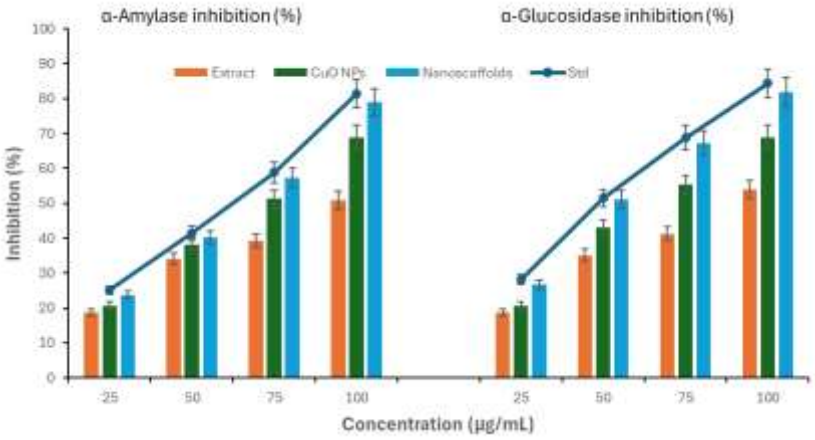

Figure 8. Antidiabetic potential of algal extract, CuO NPs and starch/PVA/CuO-NPs nanoscaffolds

The algal extract displayed moderate inhibitory activity against both enzymes. For α-amylase, inhibition increased from 18.72% at 25 µg/mL to 50.92% at 100 µg/mL, while for α-glucosidase, it ranged from 18.72% to 53.92%. These results suggest that the extract possesses antidiabetic potential, though its efficacy is lower compared to synthetic or nanoparticle-based alternatives. CuO NPs exhibited stronger inhibition than the algal extract, with α-amylase inhibition ranging from 20.72% to 68.92% and α-glucosidase inhibition from 20.72% to 68.92%. This enhanced activity can be attributed to the catalytic properties of nanoparticles, which may disrupt enzyme function more effectively than organic compounds alone. The starch/PVA/CuO-NPs nanoscaffolds outperformed both the algal extract and CuO NPs, achieving inhibition levels of 23.72% to 78.92% for α-amylase and 26.72% to 81.92% for α-glucosidase. This superior performance is likely due to the synergistic effects of the nanocomposite structure, which enhances enzyme interaction and may provide controlled release of active components. This study highlights the potential of nanoscaffolds as a promising antidiabetic agent, combining the benefits of CuO NPs with a supportive polymeric matrix. While the algal extract shows moderate activity, the nanoscaffolds and CuO NPs offer more potent alternatives. Further research, including in vivo studies, is needed to validate these findings and explore their therapeutic applications.

4. DISCUSSION

The successful synthesis and characterization of CuO NPs using Ectocarpales extract, and their integration into starch/PVA-based nanoscaffolds, were comprehensively validated through a range of physicochemical techniques. These results not only confirm the nanostructure's formation but also highlight its potential for biomedical applications, especially in managing diabetes through enzyme inhibition [46].

The UV–Visible absorption spectra offered initial confirmation of nanoparticle synthesis. The Ectocarpales extract displayed a broad peak around 300 nm, commonly associated with phenolic and flavonoid compounds, which absorb due to π–π* transitions. These organic constituents are typically involved in the reduction and stabilization of metal ions during green synthesis. Conversely, the CuO NPs showed a prominent absorption peak near 200 nm. This shift toward the lower UV region is characteristic of inorganic nanoparticles and suggests the successful conversion of copper precursors into nanoscale oxide particles. The sharp UV absorption also hints at a potential surface plasmon resonance effect, typical of metal and metal oxide nanoparticles, and further confirms their distinct optical identity compared to the crude extract [47].

Fourier Transform Infrared analysis highlighted the major functional groups involved in nanoparticle stabilization and scaffold integration. For the CuO NPs, the presence of O–H stretching vibrations and a Cu–O bond at around 860 cm^{-1} substantiated the formation of copper oxide. These bands suggest partial surface capping by biomolecules from the Ectocarpales extract. The nanoscaffold's spectrum displayed broader and more complex peaks, particularly the N–H and O–H stretches near 3298 cm^{-1}, and C=O and C–N vibrations, confirming the inclusion of polymeric materials (starch/PVA) and their interaction with the nanoparticles. The appearance of glycosidic and inorganic-polymer interaction peaks supported the hypothesis of a well-integrated nanocomposite structure [48].

XRD patterns substantiated the crystalline nature of the synthesized CuO NPs, which showed sharp diffraction peaks corresponding to a monoclinic tenorite phase, aligning well with the standard JCPDS file. The clarity and narrow full-width at half-maximum (FWHM) of these peaks emphasized the high crystallinity of the nanoparticles. In contrast, the nanoscaffold displayed broader and fewer peaks, indicative of a semi-crystalline nature—a typical feature of polymeric materials. The reduction in crystallinity in the nanoscaffolds can be attributed to the homogeneous dispersion of CuO NPs, which disrupts the ordered polymer chain alignment. Importantly, the absence of any new or unexpected peaks in the nanoscaffold confirmed the structural integrity of both CuO and the polymer matrix [49].

Morphological analysis using SEM provided detailed insight into the shape, size, and distribution of the CuO NPs and the nanofibrous matrix [55]. The CuO NPs appeared mostly spherical with minor irregularities and diameters ranging from 50 to 200 nm. Slight agglomeration was observed, likely due to surface charge effects, yet individual particles remained distinguishable. The nanoscaffold exhibited an interconnected, porous, and fibrous architecture with fiber diameters between 70 and 90 nm. Embedded nanoparticles were visibly dispersed throughout the matrix, confirming effective integration without significant aggregation. Such porosity and uniform dispersion are critical for applications requiring material interaction with biological environments, such as wound healing or tissue regeneration [50].

TGA results underscored the thermal stability of the nanoscaffolds. Initial weight loss below 100°C indicated water evaporation, while the major degradation points at around 337°C corresponded to the decomposition of the polymeric matrix. The total weight loss of 31.1% and the remaining stable residue reflect the thermal robustness of the composite. This residual mass, attributed to CuO content, is essential for applications that require materials to maintain their structural integrity under physiological or elevated temperature conditions [51].

The hydrodynamic size distribution showed a trimodal profile, indicating the coexistence of well-dispersed nanoparticles and minor aggregation. The mean size (Z-average) of 79.8 nm with a moderate PDI of 0.475 suggests that while aggregation occurs, the suspension retains a relatively consistent size distribution. Zeta potential values, particularly the +14.03 mV average, indicated a moderately stable colloidal system with positive surface charges. This cationic nature could enhance electrostatic interactions with negatively charged biomolecules, which is advantageous in biomedical systems. The observed surface charge may be due to residual biomolecules acting as capping agents during the green synthesis process [52].

Functional assessment through α-amylase and α-glucosidase inhibition assays revealed the therapeutic potential of the prepared materials. The Ectocarpales extract demonstrated moderate inhibitory effects, likely due to the presence of flavonoids and phenolics [6]. CuO NPs showed stronger inhibition, indicating that nanoparticles could interfere more effectively with enzyme active sites. Notably, the nanoscaffolds outperformed both, reflecting a synergistic effect of CuO NPs and the polymer matrix, which may offer controlled release and enhanced bioavailability. Their inhibition values closely approached those of the standard drug, acarbose, underscoring their potential as alternative antidiabetic agents [53].

Altogether, these results validate the successful green synthesis of CuO NPs and their efficient incorporation into a nanoscaffold system. The composite demonstrated suitable morphological, structural, thermal, and biological properties, indicating its applicability in biomedical fields, especially for antidiabetic interventions. Future studies may focus on in vivo evaluations and controlled drug release mechanisms to expand its clinical utility.

5.CONCLUSION

This study successfully demonstrated the green synthesis of CuO NPs using bioactive compounds from Ectocarpales algae, followed by their incorporation into starch/PVA nanoscaffolds for antidiabetic applications. The algal extract served as an effective reducing and stabilizing agent, facilitating the formation of crystalline CuO NPs with a monoclinic tenorite phase, as confirmed by XRD. UV-Vis spectroscopy revealed characteristic absorption peaks, while FT-IR analysis identified key functional groups involved in nanoparticle stabilization. SEM imaging confirmed the spherical morphology of CuO NPs (50–200 nm) and the uniform fibrous structure of the nanoscaffolds (70–90 nm fiber diameter), with well-dispersed nanoparticles. TGA analysis indicated thermal stability, with major degradation occurring at 337°C, while DLS and zeta potential measurements revealed moderate colloidal stability with a positive surface charge (+14.03 mV). The antidiabetic potential was evaluated through α-amylase and α-glucosidase inhibition assays. The algal extract exhibited moderate enzyme inhibition (18.72–53.92%), while CuO NPs showed enhanced activity (20.72–68.92%), likely due to their catalytic properties. The starch/PVA/CuO-NPs nanoscaffolds demonstrated the highest inhibition (23.72–81.92%), approaching the efficacy of the standard drug acarbose. This superior performance is attributed to the synergistic effects of CuO NPs and the polymeric matrix, which may enhance enzyme interaction and enable controlled release. These findings highlight the potential of algal-mediated CuO NPs and their nanocomposites as promising antidiabetic agents. The eco-friendly synthesis, combined with the structural and functional advantages of the nanoscaffolds, positions them as viable alternatives to conventional treatments. Future research should focus on in vivo studies to validate therapeutic efficacy, optimize biocompatibility, and explore scalable production methods for clinical applications. This work contributes to the growing field of green nanotechnology and its role in sustainable biomedical solutions.

Ethical Declaration: Not applicable for this study.

Funding: Not available for this study.

Conflicts of Interest: The authors declare no conflicts of interest.

Data Availability Statement: The full dataset of physiochemical characterization associated with this work is published in Mendeley Data [Dataset] Structural and functional profiling of starch-polymer nanoscaffolds enhanced with Ectocarpales-derived biogenic copper oxide nanoparticles (DOI: 10.17632/m7jzmb7mr9.1). Disclosure: The material characterization data and figures (e.g., UV, SEM, FTIR, XRD, TGA, Zeta Potential and particle sizer) presented here were generated from a common dataset and are being reused across multiple related studies on nanomaterials. All biological analyses and conclusions are original to each manuscript.

REFERENCES

1. Zhao X, An X, Yang C, Sun W, Ji H, Lian F. The crucial role and mechanism of insulin resistance in metabolic disease. Frontiers in endocrinology. 2023;14:1149239.

2. Pei J, Kumarasamy RV, Jayaraman S, Kanniappan GV, Long Q, Palanisamy CP. Quercetin-functionalized nanomaterials: Innovative therapeutic avenues for Alzheimer's disease management. Ageing Research Reviews. 2025; 104: 102665.

3. Jayaraman S, Prasad M, Natarajan SR, Krishnamoorthy R, Alshuniaber MA, Gatasheh MK, Veeraraghavan VP, Rajagopal P, Palanisamy CP. Molecular mechanisms underlying the effects of beta-sitosterol on TGF-β1/Nrf2/SIRT1/p53-mediated signaling in the kidney of a high-fat diet and sucrose-induced type-2 diabetic rat. Chemico-Biological Interactions. 2025; 411: 111443.
4. Huang Y, Guo H, Liu Y, Jin W, Palanisamy CP, Pei J, Oz F, El-Aty AMA. Effects of Natural Polysaccharides on the Gut Microbiota Related to Human Metabolic Health. Molecular Nutrition & Food Research. 2025; e202400792.
5. Prabhakaran P, Palanisamy CP, Shanmugam A, Damodharan P, Swaminathan H, Devaraj D, Ahalliya RM, Kanniappan GV. Isolation, structural characterization, and molecular docking studies on the bioactive compound from n-Hexane extract of Emilia sonchifolia (L.) DC against the pancreatic cancer target Aurora 2 Kinase. Journal of Complementary and Integrative Medicine. 2024; 22(1): 0290.
6. Jiang H, Kumarasamy RV, Pei J, Raju K, Kanniappan GV, Palanisamy CP. Integrating engineered nanomaterials with extracellular vesicles: Advancing targeted drug delivery and biomedical applications. Frontiers in Nanotechnology. 2024; 6: 1513683.
7. Guo H, Liu Y, Wan T, Song D, Palanisamy CP, Geng J, Pei J, Özmen S, El-Aty AMA. Toward personalized cancer management: Role of precision nutrition–diet interventions. Journal of Functional Foods. 2024; 123: 106584.
8. Natarajan SR, Krishnamoorthy R, Alshuniaber MA, Al-Anazi KM, Farah MA, Rajagopal P, Palanisamy CP, Veeraraghavan VP, Jayaraman S. Identification of FOXM1 as a novel protein biomarker and therapeutic target for colorectal cancer progression: Evidence from immune infiltration and bioinformatic analyses. International Journal of Biological Macromolecules. 282 (Part 4): 137201.
9. Rajendran MS, Jayaraman S, Khan JM, Jasmine S, Prabhakaran RK, Raju MV, Chandrasekaran MK, Ahalliya RM, Kannappan P, Palanisamy CP, Kanniappan GV. Investigating the colon toxicity and carcinogenic role of monosodium glutamate compared with Dimethylhydrazine in male Wistar rats: Exploring the link to childhood colon cancer risk. Journal of King Saud University - Science. 2024; 36(11): 103507.
10. Kumarasamy RV, Natarajan PM, Umapathy VR, Roy JR, Rab SO, Saeed M, Panagal M, Mironescu M, Srinivasan GP, Palanisamy CP. Clinical Applications and Therapeutic Potentials of Advanced Nanoparticles: A Comprehensive Review on Completed Human Clinical Trials. Frontiers in Nanotechnology. 2024; 6:1479993.
11. Jin W, Pei JJ, Roy JR, Jayaraman S, Ahalliya RM, Kanniappan GV, Mironescu M, Palanisamy CP. Comprehensive review on single-cell RNA sequencing: A new frontier in Alzheimer's disease research. Ageing Research Reviews. 2024; 274: 102454.
12. Pei J, Palanisamy CP, Jayaraman S, Natarajan PM, Umapathy VR, Roy JR, Panagal M, Jayaraman S. Curcumin-loaded polymeric nanomaterials as a novel therapeutic strategy for Alzheimer's disease: A comprehensive review. Ageing Research Reviews. 2024; 99: 102393.
13. Pei J, Palanisamy CP, Jayaraman S, Natarajan PM, Umapathy VR, Roy JR, Thalamati D, Ahalliya RM, Kanniappan GV*, Mironescu M. A comprehensive review on starch-based Sustainable Edible Films Loaded with Bioactive Components for Food Packaging. International Journal of Biological macromolecules. 2024; 274 (Part-1): 133332.
14. Palanisamy CP, poompradub S, Sansanaphongpricha K, Subramani K, Sonsudin F. Increased expression levels of PDGF and VEGF magnify the wound healing potential facilitated by biogenic synthesis of silver nanoparticles. Nano-Structures & Nano-Objects. 2024; 39: 101236.
15. Pei J, Palanisamy CP, Jayaraman S, Natarajan PM, Umapathy VR, Roy JR, Thalamati D, Ahalliya RM, Kanniappan GV, Mironescu M. Proteomics Profiling of Extracellular Vesicle for Identification of Potential Biomarkers in Alzheimer's Disease: A Comprehensive Review. Ageing Research Reviews. 2024; 99: 102359.
16. Xi J, Wang T, Xian P, Liu X, Du M, Yang H, Palanisamy CP, Lin W, Long Q. Proteomic insights uncover enhanced neurotherapeutic potential in conditioned mesenchymal stem cell-derived extracellular vesicles. Extracellular Vesicle. 2024; 3: 100037.
17. Pei J, Natarajan PM, Umapathy VR, Swamikannu B, Sivaraman NM, Krishnasamy L, Palanisamy CP. Advancements in the synthesis and functionalization of zinc oxide-based nanomaterials for enhanced oral cancer therapy. Molecules. 2024; 29(11): 2706.
18. Gatasheh MK, Natarajan SR, Krishnamoorthy R, Alsulami TS, Rajagopal P, Palanisamy CP, Veeraraghavan VP, Jayaraman S. Molecular analysis to identify novel potential biomarkers as drug targets in colorectal cancer therapy: an integrated bioinformatics analysis. Molecular and Cellular Oncology. 2024; 11(1): 2326699.
19. Pei J, Yan Y, Jayaraman S, Rajagopal P, Natarajan PM, Umapathy VR, Gopathy S, Roy JR, Sadagopan CS, Thalamati D, Palanisamy CP, Mironescu M. A review on advancements in the application of starch-based nanomaterials in biomedicine: Precision drug delivery and cancer therapy. International Journal of Biological Macromolecules. 2024; 130746.
20. Pei JJ, Yan Y, Palanisamy CP, Jayaraman S, Natarajan PM, Umapathy VR, Gopathy S, Roy JR, Sadagopan JC, Thalamati D, Mironescu M. Materials-based drug delivery approaches: Recent advances and future perspectives. Green Processing and Synthesis. 2024; 13: 20230094.
21. Panneerselvam S, Viswaja K, Deepa E, Prathiba S, Rebecca FS, Nivedha RP, Rajagopal P, Veeraraghavan VP, Sridevi G, Palanisamy CP, Jayaraman S. Hypoglycemic Potential of Acalypha indica in Streptozotocin-Induced Type 2 Diabetic Rats. International Journal of Drug Delivery Technology. 2026; 16(26s):1038-1047.
22. Panneerselvam S, Viswaja K, Prathiba S, Rebecca FS, Nivedha RP, Rajagopal P, Fathima SJH, Veeraraghavan VP, Sridevi G, Palanisamy CP, Jayaraman S. Acalypha Indica Attenuates Insulin Resistance in STZ-Induced Type 2 Diabetic Male Rats: Mechanistic Study. International Journal of Drug Delivery Technology. 2026; 16(26s):1027-1037.

23. Manju NE, Natarajan A, Rebecca FS, Nivedha RP, Hemalatha R, Rajagopal P, Murali R, Veeraraghavan VP, Sridevi G, Palanisamy CP, Jayaraman S. Effect of Seendhil polyherbal formulation in attenuating type-2 diabetes in STZ-induced experimental rats. International Journal of Drug Delivery Technology. 2026; 16(26s):981-989.
24. Manju NE, Natarajan A, Rebecca FS, Nivedha RP, Hemalatha R, Rajagopal P, Murali R, Veeraraghavan VP, Sridevi G, Palanisamy CP, Jayaraman S. Molecular mechanism to identify the effects of Seendhil polyherbal preparation on IRS-1/AKT/GLUT4/NRF2-KEAP-1 mediated signaling in SFZ-induced type-2 diabetic adult male rats. International Journal of Drug Delivery Technology. 2026;16(26s):972-980.
25. Palanisamy CP, Poompradub S, Sansanaphongpricha K, Jayaraman S, Subramani K, Sonsudin F. Biosynthesis of silver nanoparticles (AgNPs) using ethanolic extract of Nigella sativa (L.) seeds promotes wound healing via PDGF and VEGF signalling pathways activation. Biocatalysis and Agricultural Biotechnology. 2023; 54: 102970.
26. Palanisamy CP, Pei JJ, Phaniendra A, Venkata AAN, Jayaraman S, Veeraragahavan VP, Sridevi G, Roy JR, Janaki CS, Thalamati D, Mironescu M, Luo Q, Chai Y, Long Q. New Strategy of Neurodegenerative Disease Treatment with Extracellular Vesicles (EVs) Derived from Mesenchymal Stem Cells (MSCs). Theranostics. 2023; 13(12):4138-4165.
27. Smith DL, Orlandella RM, Allison DB, Norian LA. Diabetes medications as potential calorie restriction mimetics—a focus on the alpha-glucosidase inhibitor acarbose. GeroScience. 2021; 43:1123-33.
28. Surendran N, Chandrasekaran G, Raju MV, Chandrasekaran MK, Ahalliya RM, Palanisamy CP, Kanniappan GV, Arcot R, Alharbi NS, Thiruvengadam M. Anti-inflammatory potential of ethanolic extract of Maranta arundinacea L.: Insights from COX-2 modulation and oxidative stress analysis. South African Journal of Botany. 2026; 195: 142-151.
29. Pei J, Senthilkumar MV, Hessini K, Subramaniyam S, Sivaramakrishnan R, Kanniappan GV, Jayaraman S, Palanisamy CP. Green fabrication of starch/PVA/CuO nanoscaffolds using marine macroalgae extract for enhanced anti-inflammatory activity. Sustainable Chemistry and Pharmacy. 2026; 51: 102397.
30. Balasubramanian V, Loganathan L, Muthuswamy K, Viswanathan TM, Raju MV, Chandrasekaran MK, Ahalliya RM, Poorasamy J, Palanisamy CP, Dominic S, Kanniappan GV. Anticancer therapeutic efficacy of PEGylated β-galactosidase from Aspergillus terreus in DMBA-induced breast cancer: Toxicological, molecular and histopathological evaluation in Wistar rats. International Journal of Biological Macromolecules. 2026; 360: 151856.
31. Jayaraman S, Eswaran A, Rajagopal P, Palanisamy CP, Veerakumar P, Veeraraghavan VP, Sirasanagandla SR. Neuroendocrine-associated epigenetic factors in cellular senescence: mechanisms and therapeutic implications. Biogerontology. 2026; 27(2): 64.
32. Ponnusamy B, Rajagopal P, Palanisamy CP, Veeraraghavan VP, Jayaraman S. Mechanistic Exploration of the anticancer activity of Justicia adhatoda Plant Leaf Ethanolic Extract against Colon Cancer Cells: An in silico and in vitro Approach. Asian Pacific Journal of Cancer Prevention. 2026; 27(3): 1069-1080.
33. Pei J, Saran VS, Sivaramakrishnan R, Kanniappan GV, Pandurangan V, Jayaraman S, Dhayalan VK, Mironescu M, Mironescu ID, Palanisamy CP. Ultrasonic-assisted, Sargassum ilicifolium (brown marine macroalgae)-mediated biogenic synthesis of CuO nanoparticles incorporated in starch/PVA electrospun nanoscaffolds: In vitro safety and antioxidant efficacy assessment. Bioorganic Chemistry. 2026; 173: 109679.
34. Raj MAPA, Subramaniyam S, Kanniappan GV, Jayaraman S, Palanisamy CP. Sustainable fabrication of starch/PVA/CuO electrospun nanoscaffolds from Turbinaria ornata (marine macroalgae) extract: Physicochemical characterization and antidiabetic evaluation. Kuwait Journal of Science. 2026; 53(2): 100545.
35. Pei J, Ganesh NS, Subramaniyam S, Sivaramakrishnan R, Kanniappan GV, Jayaraman S, Palanisamy CP. Sustainable fabrication of starch/PVA/CuO electrospun nanoscaffolds from Padina tetrastromatica (Brown macroalgae) extract: Physicochemical characterization and antidiabetic assessment. Sustainable Chemistry One World. 2026; 9: 100195.
36. Sakthiraj A, Sivaramakrishnan R, Subramaniyam S, Kanniappan GV, Pandurangan V, Jayaraman S, Dhayalan VK, Mironescu M, Mironescu ID, Palanisamy CP. Chemical Physics Impact. Starch/PVA electrospun nanoscaffolds loaded with ultrasonic-assisted green-synthesis of CuO nanoparticles from marine macroalgae (Gracilaria corticata) extract: Cytotoxicity and antioxidant analysis. 2026; 12: 101018.
37. Raju M, Chandrasekaran MK, Loganathan L, Ahalliya RM, Mironescu M, Mironescu ID, Palanisamy CP, Kanniappan GV. Lipid remodeling and ferroptosis in phosphatidylcholine-mediated tumor–stroma crosstalk. Frontiers in Molecular Biosciences. 2026; 13: 1742305.
38. Kunamalla R, Panagal M, Palanisamy CP. Biogenic synthesis and fabrication of starch/PVA/CuO electrospun nanoscaffolds from Sargassum ilicifolium (brown marine macroalgae) extract for anticancer activity on HT-29 and MCF-7 cancer cells. Biocatalysis and Agricultural Biotechnology. 2026; 72: 103923.
39. Pei J, Govindaraj H, Sivaramakrishnan R, Kanniappan GV, Pandurangan V, Dhayalan VK, Mironescu M, Mironescu ID, Jayaraman S, Palanisamy PC. Sustainable fabrication of biopolymer-based (starch/PVA) nanoscaffolds loaded with green-synthesized CuO nanoparticles from Sargassum wightii (marine macroalgae): Cytocompatibility and antioxidant activity. Biomaterials Advances. 2026; 182: 214660.
40. Pei J, Perumal NC, Meng P, Long Q, Palanisamy CP. Extracellular vesicle-based biosensors for Alzheimer's disease: A new frontier in precision diagnostics. Ageing Research Reviews. 2026; 113: 102904.
41. Shree P, Sivaramakrishnan R, Kanniappan GV, Pandurangan V, Jayaraman S, Dhayalan VK, Mironescu M, Mironescu ID, Palanisamy CP. Antioxidant and biocompatible CuO-starch/PVA nanoscaffolds via ultrasonic green synthesis using Turbinaria conoides (brown marine macroalgae). Medicine in Drug Discovery. 2025; 28: 100238.
42. Gong J, Lin J, Guan T, Pei J, Palanisamy CP, El-AtyFrom AMA. selenium tolerance to nanoplastic antagonism: Comprehensive characterization of L. casei SNUT1 and its extracellular vesicle–nanoselenium complex. Food Bioscience. 2025; 74: 107749.

43. Poochi SP, Sundarraj R, Raju MV, Chandrasekaran MK, Ahalliya RM, Palanisamy CP, Kanniappan GV, Kondapavuluri BK, Thiruvengadam M. Harnessing Nature: Computational and Experimental Insights Into Ipomoea obscura Metabolites for Bladder Cancer Therapy. Chemistry and Biodiversity. 2025; 0: e00909.
44. Dugganaboyana GK, Kannankumar MKG, Shivaramakrishna S, Raju MV, Chandrasekaran MK, Ahalliya RM, Panneerselvam N, Palanisamy CP, Kanniappan GV. Phytochemical insights, antioxidant activity and therapeutic potential of Cassia senna against prostate cancer in Wistar albino rats. Discover Applied Sciences. 2025; 7:1206.
45. Natarajan SR, Krishnamoorthy R, Alshuniaber MA, Gatasheh MK, Rajagopal P, Veeraraghavan VP, Palanisamy CP, Jayaraman S. KDM1A Facilitates Oncogenic Potential in Colorectal Cancer Progression Through the Activation of AXIN/GSK3β/β-Catenin Signaling Pathways: Evidence From Integrated Transcriptomics and In Vitro Studies. The Journal of Gene Medicine. 2025; 27(11): e70053.
46. Guan T, Gong J, Lin J, Palanisamy CP, Jinjin Pei J, El-Aty AMA. Machine learning-driven multimodal optimization of selenium biotransformation and flavor profiling in fermented apple–Yacon functional beverages. Innovative Food Science & Emerging Technologies. 2025; 105: 104198.
47. Natarajan SR, Krishnamoorthy R, Alshuniaber MA, Alsulami TS, Gatasheh MK, Rajagopal P, Palanisamy CP, Govindan R, Veeraraghavan VP, Jayaraman S. ABCE1 facilitates tumour progression via aerobic glycolysis and inhibits cell death in human colorectal cancer cells through the p53 signalling pathway. Scientific Reports. 2025; 15: 24674.
48. Huang Y, Guo H, Liu Y, Jin W, Palanisamy CP, Pei J, Oz F, El-Aty AMA. Effects of Natural Polysaccharides on the Gut Microbiota Related to Human Metabolic Health. Molecular Nutrition & Food Research. 2025; 69:e202400792.
49. Poornima K, Meenakshi K.C, Manikandan V.R, Shankari G, Prabhu D, Rathi M.A, Palanisamy CP, Balaji R, Gopalakrishnan V.K. Exploring the anticancer potential of Jerantinine A from Tabernaemontana coronaria against prostate, breast, and ovarian cancers: A computational approach. Journal of Complementary and Integrative Medicine, 2025 22(2): 363–372.
50. Palanisamy CP, Poompradub S, Sansanaphongpricha K, Jayaraman S, Subramani K. Faridah Sonsudin gGreen synthesis of Nigella sativa-mediated silver nanoparticles for enhanced antibacterial activity and wound healing: Mechanistic insights and biomedical applications. Environmental Nanotechnology, Monitoring & Management. 2025; 24: 101085.
51. Surendran N, Raju MV, Chandrasekaran MK, Ahalliya RM, Palanisamy CP, Chandrasekaran G, Kanniappan GV. Physicochemical characterization of starch from Maranta arundinacea L.(arrowroot) rhizomes and its inhibition of COX-2: In vivo validation. Bioactive Carbohydrates and Dietary Fibre. 2025; 33: 100465.
52. Kannappan P, Chandrasekaran MK, Raju MV, Gopalakrishnan S, Dhamodharan P, Ahalliya RM, Palanisamy CP, Raju B, Kanniappan GV. Exploring the anticancer potential of Jerantinine A from Tabernaemontana coronaria against prostate, breast, and ovarian cancers: a computational approach. Journal of Complementary and Integrative Medicine. 2025; 22(02): 363-372.
53. Radulescu D-M, Surdu V-A, Ficai A, Ficai D, Grumezescu A-M, Andronescu E. Green synthesis of metal and metal oxide nanoparticles: a review of the principles and biomedical applications. International journal of molecular sciences. 2023; 24(20):15397.